Lower lower-critical spin-glass dimension from quenched mixed-spatial-dimensional spin glasses

Bora Atalay[1] and A. Nihat Berker[2,3]
[1]*Faculty of Engineering and Natural Sciences, Sabancı University, Tuzla, Istanbul 34956, Turkey*
[2]*Faculty of Engineering and Natural Sciences, Kadir Has University, Cibali, Istanbul 34083, Turkey*
[3]*Department of Physics, Massachusetts Institute of Technology, Cambridge, Massachusetts 02139, USA*

(Received 16 August 2018; published 15 October 2018)

By quenched-randomly mixing local units of different spatial dimensionalities, we have studied Ising spin-glass systems on hierarchical lattices continuously in dimensionalities $1 \leqslant d \leqslant 3$. The global phase diagram in temperature, antiferromagnetic bond concentration, and spatial dimensionality is calculated. We find that, as dimension is lowered, the spin-glass phase disappears to zero temperature at the lower-critical dimension $d_c = 2.431$. Our system being a physically realizable system, this sets an upper limit to the lower-critical dimension in general for the Ising spin-glass phase. As dimension is lowered towards d_c, the spin-glass critical temperature continuously goes to zero, but the spin-glass chaos fully subsists to the brink of the disappearance of the spin-glass phase. The Lyapunov exponent, measuring the strength of chaos, is thus largely unaffected by the approach to d_c and shows a discontinuity to zero at d_c.

DOI: 10.1103/PhysRevE.98.042125

I. INTRODUCTION: SPIN-GLASS LOWER-CRITICAL DIMENSION

The lower-critical dimension d_c of an ordering system, where the onset of an ordered phase is seen as spatial dimension d is raised, has been of interest as a singularity of a continuous sequence of singularities, the latter being the phase transitions to the ordered phase which change continuously as d is raised from d_c. The lower-critical dimension of systems without quenched randomness has been known for some time as $d_c = 1$ for the Ising-type ($n = 1$ component order-parameter) systems and $d_c = 2$ for XY, Heisenberg, etc. ($n = 2, 3, \ldots$) systems, highlighted with a temperature range of criticality at $d_c = 2$ of the XY model [1,2]. In systems with quenched randomness, a controversy on the lower-critical dimension of the random-field Ising system has settled at $d_c = 2$ [3–10]. Quenched bond randomness affects the first- versus second-order nature of the phase transition in an ordered phase that exists without quenched randomness (such as the ferromagnetic phase), rather than the dimensional onset of this ordered phase.

The situation is inherently different with an ordered phase that is caused by the quenched randomness of competing ferromagnetic-antiferromagnetic (and more recently right-left chirality or helicity [11]) interactions, namely, the Ising spin-glass phase. Replica-symmetry-breaking mean-field theory yields $d_c = 2.5$ [12], which is of immediate high interest as an example of a noninteger lower-critical dimension. The numerical fit to spin-glass critical temperatures [13] and free-energy barriers [14] for integer dimensions also suggests $d_c = 2.5$. Numerical fits to the exact renormalization-group solutions of two different families of hierarchical lattices with a sequence of decreasing dimensions yield $d_c = 2.504$ [15,16] and $d_c = 2.520$ [17], which are of further interest by being nonsimple fractions. The strength of hierarchical lattice approaches is that they present exact (numerical) solutions [18–20], but they involve nonunique continuations between integer dimensions, being based on different families of fractal graphs. However, in the hunt for the lower-critical dimension, since each hierarchical lattice constitutes a physical realization, calculating a finite-temperature spin-glass phase at d automatically pushes the lower-critical dimension to $d_c < d$, which is an important piece of information.

The exact numerical renormalization-group solution of hierarchical lattices, used in the present study, has been fully successful in all aspects of lower-critical-dimension behavior mentioned in the first paragraph of this section. Whereas previous studies with hierarchical lattices have used in each calculation a lattice with the same dimensionality at every locality (these include but are not confined to hierarchical lattices that are simultaneously approximate solutions [21,22] for hypercubic and other Euclidian lattices), we quenched-randomly mix units with local dimensionality $d = 2$ and $d = 3$. By varying the relative concentration of these two units, we continuously span from $d = 2$ to $d = 3$. In this physically realizable system, we find $d_c = 2.431$, lower than previously found values and thus setting an upper limit to the

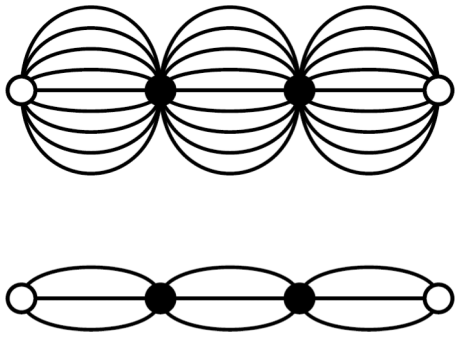

FIG. 1. Local graphs with $d = 2$ (bottom) and $d = 3$ (top) connectivity. The cross-dimensional hierarchical lattice is obtained by repeatedly imbedding the graphs in place of bonds, randomly with probability $1 - q$ and q for the $d = 2$ and $d = 3$ units, respectively.

 ©2018 American Physical Society

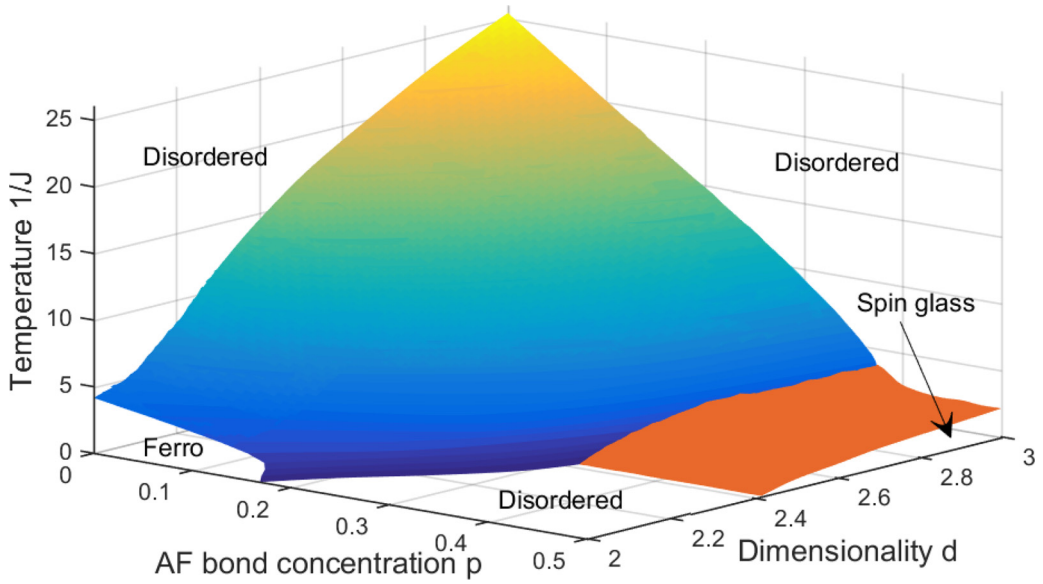

FIG. 2. Calculated exact global phase diagram of the Ising spin glass on the cross-dimensional hierarchical lattice, in temperature $1/J$, antiferromagnetic bond concentration p, and spatial dimension d. The global phase diagram is symmetric about $p = 0.5$; the mirror image portion of $0.5 < p < 1$ is not shown. The spin-glass phase is thus clearly seen, taking off from zero temperature at $d_c = 2.431$.

actual lower-critical dimension of the Ising spin-glass phase. By physically realizable system, it is meant that this lattice can actually be constructed as a physical object. In fact, this guarantees that the fundamental laws of thermodynamics are obeyed and underlies the robustness of hierarchical lattices used as an approximation for Euclidian lattices [18]. Other examples of physically realizable approximations have been used in turbulence [23], disordered alloys [24], and polymers [25,26]. Further, hierarchical lattices are more appropriate for many actual (physical) systems such as climate; internet, transportation, and neural networks; finance [27]; and DNA-binding [28] problems. By lower-critical dimension d_c of the spin-glass phase, the lowest dimension in any physically realizable system that has a spin-glass phase is meant. Such a threshold dimension of spin-glass order can be found higher (but not lower) by restricting a study to a certain class of systems, such as a given family of hierarchical lattices.

In the present study, as our spin-glass phase disappears at zero temperature at $d_c = 2.431$, it is fully chaotic, with a calculated Lyapunov exponent of $\lambda = 1.56$ (this exponent equals 1.93 at $d = 3$), which is in sharp contrast to the disappearance, as frustration is microscopically turned off, of the spin-glass phase to the Mattis-gauge-transformed ferromagnetic phase, where the Lyapunov exponent (and chaos) continuously goes to zero [29]. In the present work we also obtain a global phase diagram in the variables of temperature, antiferromagnetic bond concentration, and spatial dimensionality.

II. MODEL AND METHOD: MOVING BETWEEN SPATIAL DIMENSIONS THROUGH LOCAL DIFFERENTIATION

The Ising spin-glass system has the Hamiltonian

$$-\beta\mathcal{H} = \sum_{\langle ij \rangle} J_{ij} s_i s_j, \tag{1}$$

where $\beta = 1/kT$, at each site i of the lattice the spin $s_i = \pm 1$, and $\langle ij \rangle$ denotes summation over all nearest-neighbor site pairs. The bond J_{ij} is ferromagnetic $J > 0$ or antiferromagnetic $-J$ with respective probabilities $1 - p$ and p. This Hamiltonian is lodged on the hierarchical lattice constructed with the two graphs shown in Fig. 1. The lower graph has a length rescaling factor (distance between the external vertices) of $b = 3$ and a volume rescaling factor (number of internal bonds) of $b^d = 9$. Thus, self-imbedding the lower graph into its bonds *ad infinitum* results in a $d = 2$ spatial dimensional lattice that is numerically exactly soluble. The upper graph similarly yields $d = 3$. Other graphs have been used to systematically obtain intermediate noninteger dimensions [17].

For recent exact calculations on hierarchical lattices, see Refs. [27,28,30–36]. Thus, previous works have generally used a hierarchical lattice generated by a single graph and spatial dimensionality that is microscopically uniform throughout the system. By contrast, we mix the two graphs with local $d = 2$ and $d = 3$ in frozen randomness and definite proportionality: Starting with either graph (in the thermodynamic limit, this choice does not matter), each bond is replaced by the $d = 2$ or $d = 3$ graph, with probability $1 - q$ and q, respectively. This random imbedding is repeated *ad infinitum*. Thus, the dimensionality of the macroscopic system is $(1 - q) \times 2 + q \times 3 = 2 + q$.

The exact renormalization-group solution of this system works in the opposite direction from the lattice construction just described. As described after Eq. (1), we start with the double-valued distribution of $+J$ or $-J$ bonds, with probabilities $1 - p$ and p, respectively, on a $d = 2$ or $d = 3$ unit with probabilities $1 - q$ and q, respectively. The local renormalization-group transformation proceeds by b^{d-1} bond movings followed $b = 3$ (to preserve the ferromagnetic-antiferromagnetic symmetry) decimations, generating a distribution of 500 new interactions, which is of course no longer double valued [36]. (In fact, for numerical efficiency, these

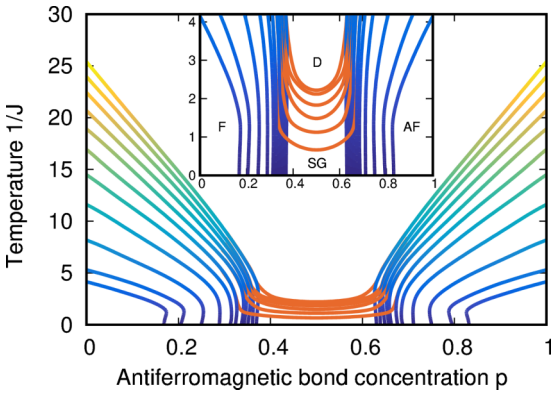

FIG. 3. Constant dimensionality d cross sections of the global phase diagram in Fig. 2. The cross sections are, starting from high temperature, for $d = 3, 2.9, 2.8, 2.7, \ldots, 2.1, 2$. It can be seen that, as the dimensionality d approaches $d_c = 2.431$ from above, the spin-glass phase disappears at zero temperature.

operations are broken down to binary steps, each involving two distributions of 500 interactions.) In the disordered phase, the interactions converge to zero. In the ferromagnetic and antiferromagnetic phases, under renormalization group, the interaction diverges to strong coupling as the renormalized average $\overline{J}' \sim b^{y_R^F}\overline{J}$, where the prime refers to the renormalized system and $y_R^F > 0$ is the runaway exponent of the ferromagnetic sink of the renormalization-group flows. In the spin-glass phase, under renormalization group, the distribution of interactions continuously broadens symmetrically in ferromagnetism and antiferromagnetism, the absolute value of the interactions diverging to strong coupling as the renormalized average $\overline{|J|}' \sim b^{y_R^{\rm SG}}\overline{|J|}$, where $y_R^{\rm SG} > 0$ is the runaway exponent of the spin-glass sink of the renormalization-group flows. The runaway exponents y_R^F and $y_R^{\rm SG}$ are given below as a function of dimensionality d. Our method has been described in detail in Refs. [11,17,29,36].

III. TRANSITIONAL DIMENSIONAL GLOBAL PHASE DIAGRAM AND FULL CHAOS EVEN AT SPIN-GLASS DISAPPEARANCE

Figure 2 shows our calculated global phase diagram in the variables of temperature $1/J$, antiferromagnetic bond concentration p, and spatial dimensionality $2 \leqslant d \leqslant 3$. In addition to the high-temperature disordered phase, ferromagnetic, antiferromagnetic (the phase diagram is ferromagnetic-antiferromagnetic symmetric about $p = 0.5$ and the mirror-image antiferromagnetic part of $p > 0.5$ is not shown; however, see Figs. 3 and 4), and spin-glass ordered phases are seen. As dimensionality d is lowered, the spin-glass phase disappears at zero temperature at the lower-critical dimension of $d_c = 2.431$. Constant-dimension d cross sections of the global phase diagram are in Fig. 3, where the gradual temperature lowering of the spin-glass phase, as the lower-critical dimension $d_c = 2.431$ is approached from above, can be seen. However, such gradual disappearance is not the case for the chaos [37–39] inherent to the spin-glass phase, as shown below.

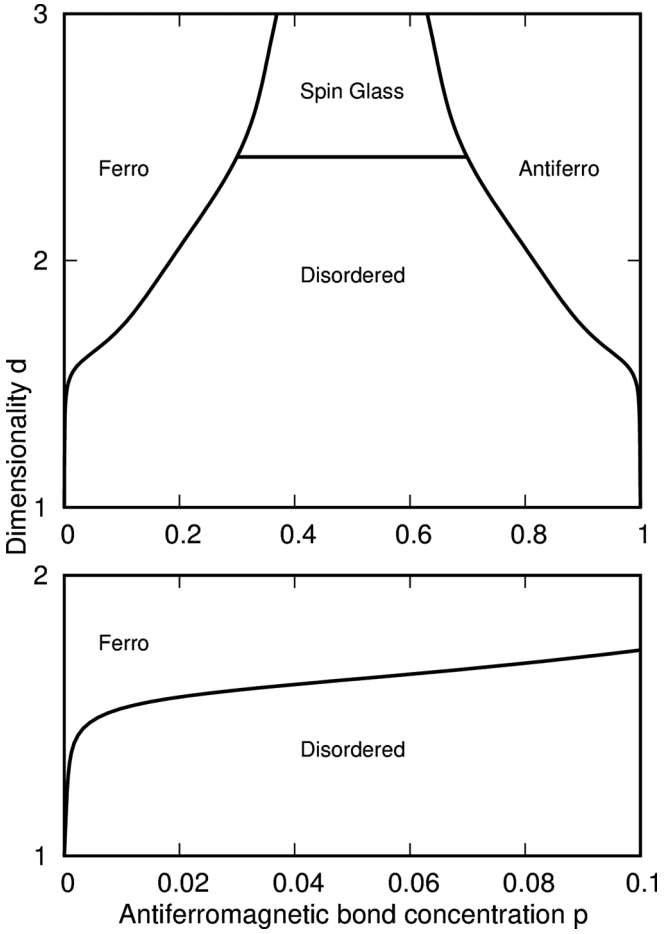

FIG. 4. Zero-temperature phase diagram of the Ising spin-glass system on the cross-dimensional hierarchical lattice, in antiferromagnetic bond concentration p and and spatial dimension d. The lower-critical dimension of $d_c = 2.431$ is clearly visible.

Figure 4 shows the calculated zero-temperature phase diagram in the variables of antiferromagnetic bond concentration p and spatial dimensionality $1 \leqslant d \leqslant 3$. For this figure, the calculation is continuously extended down to $d = 1$ by again quenched-randomly mixing our $d = 2$ graph (Fig. 1) and a linear three-segment strand. The smoothness of the boundaries at $d = 2$ validates our method. The independence of d_c from p is noteworthy.

An inherent signature of the spin-glass phase is the chaotic behavior [37–44] of the interaction at a given locality as a function of scale change, namely, under consecutive renormalization-group transformations. This chaos is shown in Fig. 5 for a variety of dimensions, including the lower-critical dimension $d_c = 2.431$. For each chaos, the Lyapunov exponent

$$\lambda = \lim_{n\to\infty} \frac{1}{n} \sum_{k=0}^{n-1} \ln \left| \frac{dx_{k+1}}{dx_k} \right|, \tag{2}$$

where $x_k = J(ij)/\overline{|J|}$ at step k of the renormalization-group trajectory, measures the strength of the chaos and is calculated and shown for the spatial dimensions in Fig. 5. It can be seen that the system shows strong chaos (positive Lyapunov ex-

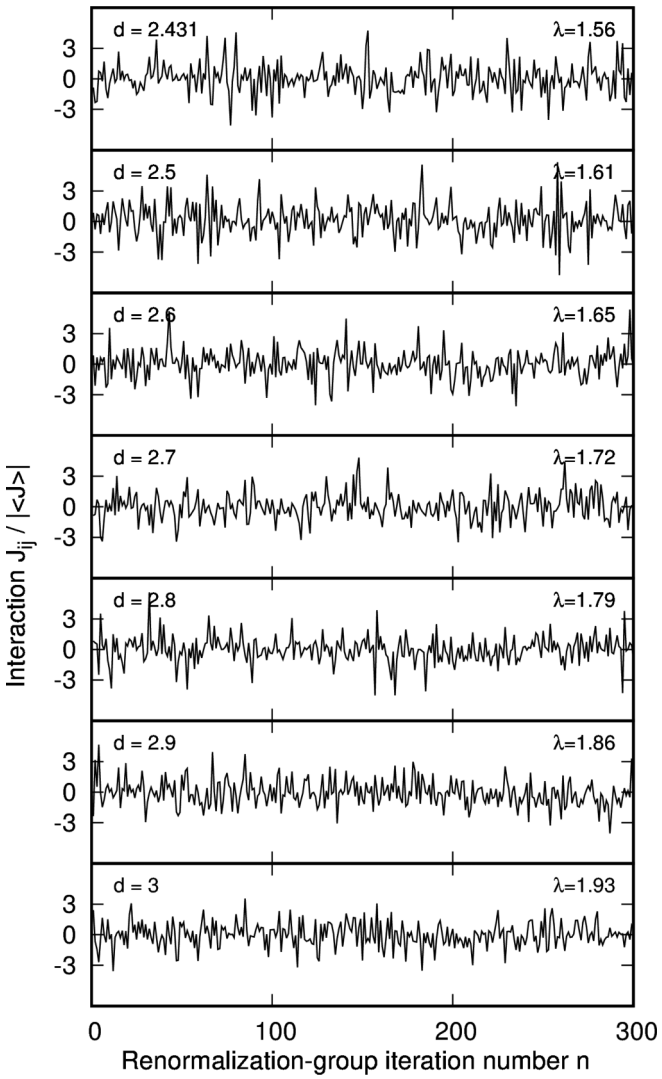

FIG. 5. Chaotic renormalization-group trajectory of the interaction J_{ij} at a given location $\langle ij \rangle$, for various spatial dimensions between the lower-critical dimension $d_c = 2.431$ and $d = 3$. Note that strong chaotic behavior, as reflected by the shown calculated Lyapunov exponents λ, nevertheless continues as the spin-glass phase disappears at the lower-critical dimension d_c, as seen in Fig. 6.

ponent $\lambda = 1.56$) even at $d_c = 2.431$, namely, at the brink of the disappearance of the spin-glass phase, after an essentially slow numerical evolution from the $d = 3$ value of $\lambda = 1.93$. This is in sharp contrast with the disappearance of the spin-glass phase, into a Mattis-gauge-transformed ferromagnetic phase, as frustration is gradually turned off microscopically, where chaos gradually disappears and the Lyapunov exponent continuously goes to zero, as shown in Fig. 6 of Ref. [29].

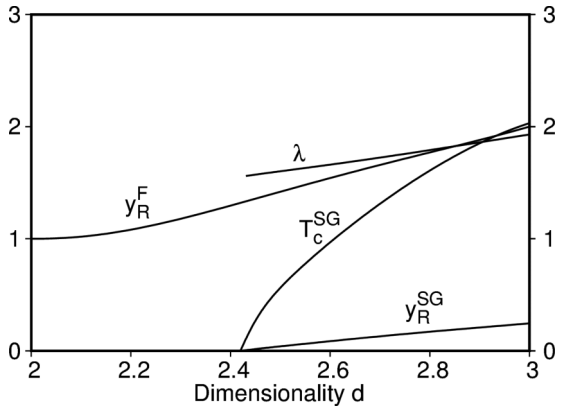

FIG. 6. Spin-glass critical temperature T_C^{SG} at $p = 0.5$, spin-glass chaos Lyapunov exponent λ, spin-glass-phase runaway exponent y_R^{SG}, and ferromagnetic-phase runaway exponent y_R^F, as a function of dimension d. Note that the ferromagnetic-phase runaway exponent y_R^F correctly tracks $d - 1$.

As shown in Fig. 6, the Lyapunov exponent, shown continuously as a function of dimension, is essentially unaffected by the disappearance of the spin-glass phase and thus shows a discontinuity at d_c. The runaway exponent of the spin-glass phase, on the other hand, correctly goes to zero at d_c, as is expected by the renormalization-group flow structure. Also shown in Fig. 6 is the spin-glass critical temperature going to zero at d_c.

IV. CONCLUSION: LOWER LOWER-CRITICAL DIMENSION AND LYAPUNOV DISCONTINUITY

By quenched-randomly mixing local units of different spatial dimensionalities, we have studied Ising spin-glass systems on hierarchical lattices continuously in dimensionalities $1 \leqslant d \leqslant 3$. We have calculated the global phase diagram in temperature, antiferromagnetic bond concentration, and spatial dimensionality. We find that, as dimension is lowered, the spin-glass phase disappears at zero temperature at $d_c = 2.431$. Our system being a physically realizable system, this sets an upper limit to the lower-critical dimension of the Ising spin-glass phase. As dimension is lowered towards d_c, the spin-glass critical temperature continuously goes to zero. The Lyapunov exponent, measuring the strength of chaos, is, on the other hand, largely unaffected by the approach to d_c and shows a discontinuity to zero at d_c.

ACKNOWLEDGMENT

Support by the Academy of Sciences of Turkey (TÜBA) is gratefully acknowledged. We thank Tolga Çağlar for most useful discussions.

[1] H. E. Stanley and T. A. Kaplan, Phys. Rev. Lett. **17**, 913 (1966).
[2] H. E. Stanley, Phys. Rev. Lett. **20**, 589 (1968).
[3] D. P. Belanger, A. R. King, and V. Jaccarino, Phys. Rev. Lett. **48**, 1050 (1982).
[4] H. Yoshizawa, R. A. Cowley, G. Shirane, R. J. Birgeneau, H. J. Guggenheim, and H. Ikeda, Phys. Rev. Lett. **48**, 438 (1982).
[5] P.-Z. Wong and J. W. Cable, Phys. Rev. B **28**, 5361 (1983).
[6] A. N. Berker, Phys. Rev. B **29**, 5243 (1984).
[7] M. Aizenman and J. Wehr, Phys. Rev. Lett. **62**, 2503 (1989).

[8] M. Aizenman and J. Wehr, Phys. Rev. Lett. **64**, 1311(E) (1990).
[9] M. S. Cao and J. Machta, Phys. Rev. B **48**, 3177 (1993).
[10] A. Falicov, A. N. Berker, and S. R. McKay, Phys. Rev. B **51**, 8266 (1995).
[11] T. Çağlar and A. N. Berker, Phys. Rev. E **96**, 032103 (2017).
[12] S. Franz, G. Parisi, and M. A. Virasoro, J. Phys. (France) I **4**, 1657 (1994).
[13] S. Boettcher, Phys. Rev. Lett. **95**, 197205 (2005).
[14] A. Maiorano and G. Parisi, Proc. Natl. Acad. Sci. USA **115**, 5129 (2018).
[15] C. Amoruso, E. Marinari, O. C. Martin, and A. Pagnani, Phys. Rev. Lett. **91**, 087201 (2003).
[16] J.-P. Bouchaud, F. Krzakala, and O. C. Martin, Phys. Rev. B **68**, 224404 (2003).
[17] M. Demirtaş, A. Tuncer, and A. N. Berker, Phys. Rev. E **92**, 022136 (2015).
[18] A. N. Berker and S. Ostlund, J. Phys. C **12**, 4961 (1979).
[19] R. B. Griffiths and M. Kaufman, Phys. Rev. B **26**, 5022 (1982).
[20] M. Kaufman and R. B. Griffiths, Phys. Rev. B **30**, 244 (1984).
[21] A. A. Migdal, Zh. Eksp. Teor. Fiz. **69**, 1457 (1975) [Sov. Phys. JETP **42**, 743 (1976)].
[22] L. P. Kadanoff, Ann. Phys. (NY) **100**, 359 (1976).
[23] R. H. Kraichnan, J. Math. Phys. **2**, 124 (1961).
[24] P. Lloyd and J. Oglesby, J. Phys. C **9**, 4383 (1976).
[25] P. J. Flory, *Principles of Polymer Chemistry* (Cornell University Press, Ithaca, 1986).
[26] M. Kaufman, Entropy **20**, 501 (2018).
[27] S. J. Sirca and M. Omladic, ARS Math. Contemp. **13**, 63 (2017).
[28] J. Maji, F. Seno, A. Trovato, and S. M. Bhattacharjee, J. Stat. Mech. (2017) 073203.
[29] E. Ilker and A. N. Berker, Phys. Rev. E **89**, 042139 (2014).
[30] N. Masuda, M. A. Porter, and R. Lambiotte, Phys. Rep. **716**, 1 (2017).
[31] S. Li and S. Boettcher, Phys. Rev. A **95**, 032301 (2017).
[32] P. Bleher, M. Lyubich, and R. Roeder, J. Math. Pures Appl. **107**, 491 (2017).
[33] H. Li and Z. Zhang, Theor. Comput. Sci. **675**, 64 (2017).
[34] J. Peng and E. Agliari, Chaos **27**, 083108 (2017).
[35] S. Boettcher and S. Li, Phys. Rev. A **97**, 012309 (2018).
[36] B. Atalay and A. N. Berker, Phys. Rev. E **97**, 052102 (2018).
[37] S. R. McKay, A. N. Berker, and S. Kirkpatrick, Phys. Rev. Lett. **48**, 767 (1982).
[38] S. R. McKay, A. N. Berker, and S. Kirkpatrick, J. Appl. Phys. **53**, 7974 (1982).
[39] A. N. Berker and S. R. McKay, J. Stat. Phys. **36**, 787 (1984).
[40] Z. Zhu, A. J. Ochoa, S. Schnabel, F. Hamze, and H. G. Katzgraber, Phys. Rev. A **93**, 012317 (2016).
[41] W. Wang, J. Machta, and H. G. Katzgraber, Phys. Rev. B **93**, 224414 (2016).
[42] L. A. Fernandez, E. Marinari, V. Martin-Mayor, G. Parisi, and D. Yllanes, J. Stat. Mech. (2016) 123301.
[43] A. Billoire, L. A. Fernandez, A. Maiorano, E. Marinari, V. Martin-Mayor, J. Moreno-Gordo, G. Parisi, F. Ricci-Tersenghi, and J. J. Ruiz-Lorenzo, J. Stat. Mech. (2018) 033302.
[44] W. Wang, M. Wallin, and J. Lidmar, arXiv:1808.00886.